JOURNAL OF VIROLOGY, Aug. 2005, p. 9933–9944 Vol. 79, No. 15
0022-538X/05/$08.00+0 doi:10.1128/JVI.79.15.9933–9944.2005
Copyright © 2005, American Society for Microbiology. All Rights Reserved.

Packaging Capacity of Adeno-Associated Virus Serotypes: Impact of Larger Genomes on Infectivity and Postentry Steps

Joshua C. Grieger and Richard J. Samulski*

Curriculum in Genetics and Molecular Biology and Gene Therapy Center, University of North Carolina at Chapel Hill, Chapel Hill, North Carolina 27599

Received 7 February 2005/Accepted 8 April 2005

The limited packaging capacity of adeno-associated virus (AAV) precludes the design of vectors for the treatment of diseases associated with larger genes. Autonomous parvoviruses, such as minute virus of mice and B19, while identical in size (25 nm), are known to package larger genomes of 5.1 and 5.6 kb, respectively, compared to AAV genomes of 4.7 kb. One primary difference is the fact that wild-type (wt) AAV utilizes three capsid subunits instead of two to form the virion shell. In this study, we have characterized the packaging capacity of AAV serotypes 1 through 5 with and without the Vp2 subunit. Using reporter transgene cassettes that range in size from 4.4 to 6.0 kb, we determined that serotypes 1 through 5 with and without Vp2 could successfully package, replicate in, and transduce cells. Dot blot analysis established that packaging efficiency was similar for all vector cassettes and that the integrity of encapsidated genomes was intact regardless of size. Although physical characterization determined that virion structures were indistinguishable from wt, transduction experiments determined that all serotype vectors carrying larger genomes (5.3 kb and higher) transduced cells less efficiently (within a log) than AAV encapsidating wt size genomes. This result was not unique to reporter genes and was observed for CFTR vector cassettes ranging in size from 5.1 to 5.9 kb. No apparent advantage in packaging efficiency was observed when Vp2 was present or absent from the virion. Further analysis determined that a postentry step was responsible for the block in infection and specific treatment of cells upon infection with proteasome inhibitors increased transduction of AAV encapsidating larger DNA templates to wt levels, suggesting a preferential degradation of virions encapsidating larger-than-wt genomes. This study illustrates that AAV is capable of packaging and protecting recombinant genomes as large as 6.0 kb but the larger genome-containing virions are preferentially degraded by the proteasome and that this block can be overcome by the addition of proteasome inhibitors.

Adeno-associated virus (AAV) is a small, single-stranded DNA dependovirus belonging to the parvovirus family. The 4.7 kb wild-type (wt) AAV genome is made up of two genes that encode four replication proteins and three capsid proteins, respectively, and is flanked on either side by 145-bp inverted terminal repeats (ITRs) (28, 37). The virion is composed of three capsid proteins, Vp1, Vp2, and Vp3, produced in a 1:1:10 ratio from the same open reading frame but from differential splicing (Vp1) and alternative translational start sites (Vp2 and Vp3, respectively) (30). Vp3 is the most abundant subunit in the virion and participates in receptor recognition at the cell surface defining the tropism of the virus. A phospholipase domain, essential for viral infectivity, has been identified in the unique N terminus of Vp1 (19, 53). The functional significance of Vp2 remains to be resolved.

Similar to wt AAV, recombinant AAV (rAAV) utilizes the *cis*-acting 145-bp ITRs to flank vector transgene cassettes, providing up to 4.5 kb for packaging of foreign DNA. Subsequent to infection, rAAV can express the therapeutic gene and persist without integration into the host genome by existing episomally in circular head-to-tail concatemers (29). Although there are numerous examples of rAAV success using this system, in vitro and in vivo, limited packaging capacity has been an impediment for AAV-mediated gene therapy of Duchenne muscular dystrophy, hemophilia A, cystic fibrosis, and other genetic diseases where the length of the coding sequence is equal in size to the wt AAV genome. For most of the larger genes mentioned above, this leaves little or no space for promoter, polyadenylation, and enhancer sequences. Recently, split vector systems, exploiting head-to-tail concatamerization formation, have been developed to circumvent the small packaging capacity of AAV genomes (13–16, 41, 52). The two approaches, *trans*-splicing and homologous recombination methods, depend upon recombination between two vector genomes (each genome encoding approximately half the transgene) within the same cell to achieve gene expression. While these approaches fundamentally solve current packaging limitations of AAV, they create some disadvantages. Cells have to be infected with numerous virus particles to increase the probability of transduction, and the system is reliant upon the efficiency of homologous recombination.

With respect to wt AAV, two groups have characterized the packaging capacity of AAV2. Hermonat et al. inserted increments of 100 bp into the wt AAV genome downstream of the capsid gene (23). Viruses carrying larger genomes (up to 5.6 kb) were able to replicate and produce infectious virions, albeit at reduced efficiency compared to wt. Dong et al. generated packaging constructs, containing a completely recombinant genome encoding the chloramphenicol acetyltransferase (CAT) gene, ranging in size from 1,918 to 6,019 bp (10). The latter studies suggest that the optimum size of AAV2 vector genomes

* Corresponding author. Mailing address: Gene Therapy Center, University of North Carolina at Chapel Hill, 7119 Thurston Bowles, CB 7352, Chapel Hill, NC 27599-7352. Phone: (919) 962-1224. Fax: (919) 966-0907. E-mail: rjs@med.unc.edu.

1
EX2012
Sarepta v. Trustees UPenn et al.
IPR2024-00580

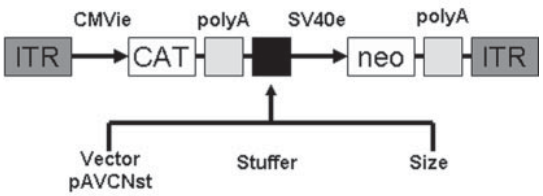

Vector pAVCNst	Stuffer	Size
D	323	4461
E	537	4675
F	622	4760
G	745	4883
H	945	5083
I	975	5113
J	1094	5232
K	1164	5302
L	1811	6019

FIG. 1. Vector sequence for the pAVCNst packaging cassettes (10). Each cassette is composed of serotype 2 ITRs with a CMV immediate-early (CMVie) promoter driving CAT gene expression. A stuffer region was designated for cloning in DNA sequences to expand the packagable genome. Letters on the left indicate different vectors. The sizes of the stuffer DNA along with total vector genome size are shown in the second and third columns, respectively.

is between 4.1 and 4.9 kb. Based on these studies, the packaging limits for AAV may differ depending on the presence of the wt AAV sequence.

Other parvoviruses have been shown to package genomes as large as 5.1 and 5.6 kb (minute virus of mice [MVM] and B19, respectively). A striking structural difference is that MVM and B19 are initially composed of two structural proteins (Vp1 and Vp2), and the N termini of the minor capsid components (Vp1 and Vp2 for B19 and Vp2 for MVM) are exposed on the surface of the virion subsequent to genome encapsidation. In contrast, the N termini of Vp1 and Vp2 of AAV are located within the virion (27, 46, 48). While Vp1 is required for infectivity, Vp2 has been shown to be nonessential (44).

Based on this evidence, we wanted to explore the possibility that producing a virion composed of only two capsid proteins may enable AAV to package larger genomes more efficiently than wt virions. We analyzed the packaging capacity of AAV serotypes 1 through 5 with and without the minor capsid subunit protein Vp2 using the previously characterized pAVCNst packaging cassettes (10) (Fig. 1). The packaging efficiency of each vector was quantitatively analyzed by dot blot hybridization, the genome size by alkaline agarose gel analysis, and transduction profile using CAT assays. In addition, similar assays were simultaneously carried out on cystic fibrosis transmembrane conductance regulator (CFTR) cassettes of various sizes. The additional transgene cassettes and the use of various AAV serotypes were utilized to determine whether the DNA sequence influenced the packaging efficiency and/or the packaging capacity of related serotypes. This study suggests that all AAV serotypes are capable of efficiently encapsidating genomes as large as 6 kb regardless of sequence, but the optimum packaging capacity is 5.23 kb. Vectors carrying larger genomes can be enhanced for more efficient transduction by the addition of proteasome inhibitors, suggesting a postentry block. The data gathered from these studies provides important information regarding AAV vector design and suggests that AAV packaging limits may not be restricted solely by the physical size of the vector template.

METHODS AND MATERIALS

Cells and viruses. HeLa, 293, and COS-1 cells were maintained at 37°C in a 5% CO_2 atmosphere in Dulbecco's modified Eagle's medium (Sigma, St. Louis, Mo.) supplemented with 10% fetal bovine serum and penicillin-streptomycin. Adenovirus dl309 has been described previously (24).

Plasmids. The AAV1 through 5 helper plasmids, pXR1 through pXR5 (32), were used in these studies. These plasmids served as the starting reagents to produce the Vp2 knockout mutant viruses ACA1 through ACA5 used in these studies. The following oligonucleotides were designed and utilized in the QuikChange multisite-directed mutagenesis kit (Stratagene) to mutate the Vp2 start codon ACG to ACA (shown in uppercase type): *AAV1ACA*, ttg agg aag gcg cta agA CAg ctc ctg gaa aga aac g; *AAV2ACA*, ttg agg aac ctg tta agA CAg ctc cgg gaa aaa aga gg; *AAV3ACA*, ttg agg aag cag cta aaA CAg ctc ctg gaa agaa agg; *AAV4ACA*, ttg agc aag cgg gtg agA CAg ctc ctg gaa aga aga gac c; *AAV5ACA*, tga aga ggg tgc taa gAC Agc ccc tac cgg aaa gc. Sequencing of miniprep DNA from each of the mutagenized pXR1 to pXR5 plasmids was then done to verify the start codon mutation. After verification, the resultant BsiWI/SwaI fragment containing the mutation was then subcloned into the respective parent plasmid. The CFTR, cytomegalovirus (CMV)-CFTR, and CMV(I)-CFTR cassettes were produced from the pBQ4.7V CFTR plasmid generously provided to us by John Olsen. This plasmid is the same as pBQ4.7 used by Drumm et al. (12), except a 450-bp piece at the end of the cDNA was replaced so there is a valine at nucleotide 1475. Briefly, AgeI and NotI restriction sites were engineered 5′ and 3′ of the CFTR gene on the pBQ4.7V plasmid utilizing the Stratagene multisite-directed PCR kit. TReGFP, with and without the simian virus 40 (SV40) intron, and the pBQ4.7V plasmid were digested with AgeI and NotI enzymes. Each digest was then PCR column purified (QIAGEN, Valencia, CA). The TReGFP digest was then treated with calf intestinal phosphatase. The TReGFP backbone and the CFTR fragment were gel extracted from the 0.7% agarose gel using the gel extraction columns from QIAGEN. The TReGFP backbone and CFTR fragment were then ligated overnight. The CFTR cassette lacking a promoter was produced by digesting the CMV(I)-CFTR cassette with KpnI and AgeI to remove the CMV and SV40 intron sequences. Klenow was then added to blunt the ends followed by self-ligation overnight.

Production of recombinant AAV utilizing the CFTR and pAVCNst packaging cassettes. To determine the effect of various genome sizes on the packaging efficiency of AAV serotypes 1, 2, 3, 4, and 5 with and without capsid subunit Vp2, we utilized the packaging plasmids pAVCNst acquired from Dong et al. (10). pAVCNst plasmids D through L were used, ranging in size from 4,461 to 6,019 bp. Each construct contains the CMV immediate-early promoter with the chloramphenicol acetyltransferase gene flanked by AAV2 ITRs. Recombinant AAV was produced using a scaled-down version of the calcium phosphate triple plasmid transfection protocol (20). One 15-cm dish of 293 cells was transfected to produce each of the viruses. Eighteen micrograms of XX6-80, 7.5 μg of helper plasmid (pXR1 to pXR5 series or the pXR1ACA to pXR5ACA series), 7.5 μg of the pAVCNst TR plasmid, 100 μl of 2.5 M $CaCl_2$, ~870 μl double-distilled water, and 1 ml of 2× HeBS buffer (20) were mixed together and subsequently added to each 15-cm dish after the calcium phosphate precipitate had formed. The cells were then harvested at 48 h posttransfection by scraping the cells from the plate. The cells were then pelleted at low-speed centrifugation (1,500 rpm), the medium was then decanted, and the cell pellet was resuspended in 3 ml of 1× phosphate-buffered saline (PBS). Three cycles of freeze-thawing in dry ice-methanol and a 37°C water bath were then performed. The cell homogenate containing the rAAV was then divided into aliquots and stored at −80°C. rAAV that was purified via CsCl gradients was produced by the calcium phosphate triple transfection method using 5- by 15-cm plates of 293 cells. Cells were scraped from each plate 48 h after transfection and pelleted by centrifugation for 5 min at 1,000 rpm in a Sorvall RT6000D centrifuge. All subsequent steps were performed on ice unless otherwise noted. The cells were then resuspended in 10 ml of double-distilled water and sonicated 25 times using a Branson Sonifier set to 50% duty and an output control of 5. One hundred microliters of DNase (10 mg/ml) was then added to the sonicated homogenate and incubated for 1 h in a 37°C water bath. CsCl (6.6 g) was then added to each sample and loaded into Beckman Quick-Seal polyallomer centrifuge tubes. The samples were then centrifuged at 65,000 rpm (402,000 × *g*) for 5 h using the Beckman NVT65 rotor in a Sorvall Ultra 80 centrifuge. Gradients were fractionated into 750-μl fractions

and stored at −20°C. AAV2 E, K, and L virus along with the CFTR vectors were produced following the triple transfection method by transfecting 15- by 15-cm plates of 293 cells, respectively. Cell homogenate was loaded onto iodixanol step gradients as described previously (55), and rAAV was isolated from the 40 to 60% interface with a syringe. rAAV2 was then purified further by fast performance liquid chromatography (FPLC) and heparin column chromatography.

Replication assays. Replication assays were carried out to determine whether the proper size genomes were being replicated from the respective pAVCNst packaging plasmids and packaged into all five AAV serotypes. 293 cells were plated into 10-cm plates and transfected with 10 μg XX680, 3.5 μg pXR2 helper plasmid, and 3.5 μg pAVCNst packaging series D through L. Replication assays were also conducted by infecting 293 cells, under conditions permissive for replication, in 10-cm plates with 1×10^9 viral genomes. 293 cells were transfected with 3.5 μg of pXR2 and 10 μg of XX680 6 h prior to infection. Cells were then harvested 42 h postinfection, and low-molecular-weight DNA was isolated by Hirt extraction. Samples were DpnI digested and fractionated on an agarose gel, transferred to a HyBond N+ nylon membrane (Amersham Biosciences), and probed overnight. This assay was used to assess the ability of rAAV to deliver its genome to the nucleus and replicate.

Titer determination of rAAV. The presence and titer determination of DNA containing viral particles was determined by DNA dot blot hybridization. Briefly, 10 μl of each viral lysate sample was treated with 50 μl of 0.1 μg/μl in 10 mM Tris (pH 7.5)–10 mM $MgCl_2$ for 1 h at 37°C. Fifty microliters of 100 mM EDTA was then added to each sample, followed by incubation at 50°C with 50 μl of proteinase K–2.5% *N*-lauryl-sarcosyl solution for 45 min. Fifty microliters of 5 M NaOH was then added to each sample and incubated for 20 min. The samples were applied to a HyBond N+ membrane (Amersham Biosciences) through the use of a dot blot manifold and probed overnight.

Electron microscopy. Peak fractions of rAAV2 E, K, and L were placed on a 400-mesh glow-discharged carbon grid by inversion on a 20-μl drop of virus. The grid was washed three times in 20 μl of PBS for 1 min. The virus was then stained for 1 min with 2% uranyl acetate. The virus was visualized by using a Zeiss EM 910 electron microscope.

Extraction of genomes from virions. DNA was extracted from each virus using equal volumes of viral lysate in the study. The virus was incubated with 50 μl of 0.1 μg/μl DNase I in 10 mM Tris (pH 7.5)–10 mM $MgCl_2$ for at least 1 h at 37°C to digest unpackaged genomes. Fifty microliters of 100 mM EDTA was then added to each sample to deactivate DNase I, followed by incubation at 50°C with 50 μl of proteinase K–2.5% *N*-lauryl-sarcosyl solution for 45 min to lyse the virus. Viral DNA was extracted twice with phenol-chloroform and then precipitated with 2 equivalent volumes of ethanol and 10% (vol/vol) 3 M sodium acetate. Alkaline agarose gel electrophoresis was then carried out as described previously (34a) to determine the size of the packaged genome. DNA size markers were produced via single digests of the K pAVCNst plasmid with EcoRI and BamHI, yielding the 4- and 5-kb-long DNAs, respectively.

CAT assays to analyze transduction efficiency. HeLa or COS-1 cells (6×10^5) were plated in each 6-cm dish for AAV serotypes 1 to 3 and 4 and 5, respectively. After the cells adhered to the dishes, they were infected with 500 genome-containing virions per cell with an adenovirus (dl309) multiplicity of infection (MOI) of 5. Cells were harvested 24 h after infection and lysed as described previously (34a). CAT assays were then carried out on the protein homogenate as described previously (34a) to assess the transduction profiles of rAAV serotypes 1 through 5 with and without capsid subunit protein Vp2.

CFTR transduction assays. rAAV2 viruses were produced by utilizing the following CFTR TR2 cassettes: (i) CFTR (5.1 kb), (ii) CMV-CFTR (5.7 kb), and (iii) CMV(I)-CFTR (5.9 kb). HeLa cells (5×10^5) were plated in the wells of six-well plates. HeLa cells were then infected with approximately 2,000 viral genomes/cell of each AAV2-CFTR vector 8 hours after seeding the wells. At 48 h postinfection, total RNA was isolated using the RNeasy column method (QIAGEN, Valencia, CA). Briefly, 350 μl of RNeasy lysis buffer (RLT plus β-mercaptoethanol) was added to the pelleted HeLa cells for resuspension and lysis. The lysate was then passed through a Qiashredder (QIAGEN). From this point, the standard minicolumn protocol was followed and RNA was eluted in 30 μl of the supplied RNase-free water. poly(A) RNA was then isolated from 15 μl of the total RNA. The Oligotex mRNA mini kit (QIAGEN, Valencia, CA) was used to isolate the mRNA from the total RNA according to protocol. mRNA was eluted from the oligonucleotide T bead suspension using 60 μl of supplied elution buffer OEB (5 mM Tris, pH 7.5). Reverse transcription (RT)-PCR was then carried out on the isolated mRNA utilizing the Superscript III first-strand system for RT-PCR (Invitrogen). Briefly, 8 μl of mRNA along with 1 μl of 50 ng/μl of random hexamers and 10 mM deoxynucleoside triphosphates were incubated at 65°C for 5 min and cooled on ice for over 1 min. Ten microliters of cDNA synthesis mix (2 μl of 10× RT buffer, 4 μl 25 mM $MgCl_2$, 2 μl 0.1 M dithiothreitol, 1 μl RNaseOUT, and 1 μl SuperScript III RT) was added to the mRNA samples and incubated at 25°C for 10 min followed by 50°C for 50 min. The reactions were terminated by heating to 85°C for 5 min. One microliter of RNaseH was then added to each tube and incubated at 37°C for 20 min. Three microliters of the cDNA was then used in standard PCR using *Taq* polymerase to determine whether CFTR transcripts were produced. To do this, primers specific for the virally delivered CFTR transcript were utilized in the PCR to detect and amplify the CFTR cDNA yielding a 450-bp fragment.

RESULTS

Packaging efficiency of AAV serotypes. In this study, we set out to characterize the packaging capacity of AAV serotypes 1 through 5 with and without capsid subunit protein Vp2. Nine CMV-driven chloramphenicol acetyltransferase pAVCNst packaging cassettes ranging in size from 4,461 to 6,019 bp were used (Fig. 1). An initial characterization of AAV serotypes encapsidating the genomes of various sizes was carried out on crude lysate virus as described in Materials and Methods to more efficiently screen the 90 different viruses. Dot blot analysis was performed on the 90 different viruses after vector production to determine whether the titer or packaging efficiency was influenced by genome size. Table 1 summarizes the range of vector titers acquired from three separate viral preparations using the nine packaging cassettes (D through L). Titers ranged from 10^6 to 10^8 viral genomes/μl for a majority of the viral preparations with little to no differences in titer between AAV produced with the largest cassettes (3×10^6 to 9×10^7 viral genomes/μl) compared to the wt size cassettes (6×10^6 to 1×10^8 viral genomes/μl). These data illustrate that there is no apparent difference in packaging efficiency among all five serotypes with and without Vp2.

Genome integrity of AAV serotypes. The dot blot method is an effective method to quantitate viral titers, but it is incapable of determining whether each AAV serotype has successfully packaged the larger transgene cassettes in their entirety. Two approaches were utilized to determine genome integrity after encapsidation: direct lysis of the viral particles and isolation of uncoated vector genomes from infected cells. In the first approach, viral DNA was isolated directly from each AAV serotype by treating the particles with DNase I to remove any unpackaged DNA, followed by lysis using proteinase K and detergent as described in Materials and Methods. The single-stranded vector genomes were extracted and analyzed on alkaline agarose gels to determine size and integrity. A representative Southern blot of an alkaline agarose gel of genomes isolated from AAV1 is shown in Fig. 2. Half of the viral samples were subjected to DNase digestion prior to genome isolation from the virions. This was done to determine whether the larger genomes were packaged in their entirety and protected from DNase. Upon comparison of DNase-treated and untreated samples of the same size, it is clear that the correct size band is present with similar intensity. We have noted the indication of DNA smearing in the DNase-treated and untreated samples in this Southern blot along with those from the other serotypes, but the smearing is not extensive and is homogeneous throughout all of the samples tested (Fig. 2, lanes 7 and 22). Based on this assay, AAV serotypes 1 through 5 are capable of packaging and protecting genomes as large as 6 kb.

Isolating DNA from AAV particles via direct lysis of the virion with the method previously described (Fig. 2) does not

TABLE 1. Dot blot titers of small-scale virus productions of each serotype with and without Vp2[a]

Packaging cassette	Titer range (viral genomes/μl) for:									
	AAV1	ACA1	AAV2	ACA2	AAV3	ACA3	AAV4	ACA4	AAV5	ACA5
D	9×10^7–3×10^8	1×10^8	3×10^7	2×10^7–1×10^8	3×10^7–2×10^8	3×10^7–2×10^8	3×10^7–1×10^8	3×10^7–1×10^8	7×10^8–2×10^7	9×10^8–2×10^7
E	3×10^7–1×10^8	1×10^7–1×10^8	6×10^8–4×10^7	6×10^8–8×10^7	1×10^7–1×10^8	6×10^8–1×10^8	2×10^7–9×10^7	1×10^8–1×10^8	2×10^8–1×10^7	9×10^5–1×10^7
F	9×10^7	3×10^7–8×10^7	3×10^7–5×10^7	2×10^7–1×10^8	3×10^7–1×10^8	9×10^8–1×10^8	6×10^8–1×10^8	2×10^7–2×10^8	9×10^6–1×10^7	9×10^8–1×10^7
G	6×10^7–2×10^8	6×10^7–1×10^8	2×10^7–7×10^7	1×10^7–1×10^8	6×10^7–3×10^8	1×10^7–3×10^8	3×10^8–9×10^7	2×10^7–1×10^8	6×10^8–1×10^7	6×10^6–1×10^7
H	3×10^7–1×10^8	6×10^7–1×10^8	9×10^8–3×10^7	6×10^7–1×10^8	3×10^7–3×10^8	3×10^7–1×10^8	6×10^8–1×10^6	9×10^8–2×10^8	3×10^8–1×10^7	3×10^8–1×10^7
I	3×10^7–1×10^8	3×10^7–1×10^8	3×10^8–4×10^7	2×10^7–8×10^7	3×10^7–2×10^8	3×10^7–2×10^8	1×10^7–2×10^8	1×10^7–2×10^8	3×10^7	2×10^7–3×10^7
J	1×10^7–3×10^7	3×10^7–9×10^7	2×10^8	6×10^8–4×10^7	9×10^8	3×10^7–1×10^8	1×10^7	3×10^8–8×10^7	9×10^6–1×10^7	1×10^7–1×10^7
K	1×10^7–2×10^7	2×10^8–7×10^7	9×10^5–7×10^7	3×10^5–5×10^7	3×10^7–1×10^8	6×10^7–3×10^8	3×10^8–5×10^7	6×10^8–1×10^8	1×10^7–3×10^7	1×10^7–3×10^7
L	9×10^8–8×10^7	3×10^7–7×10^7	3×10^6–3×10^7	6×10^7	3×10^6–7×10^7	3×10^6–9×10^7	9×10^8–7×10^7	6×10^6–2×10^7	4×10^6–1×10^7	9×10^8–1×10^7

[a] Ranges of DNase-resistant particle titers of AAV serotypes 1 through 5, with (AAV1 to AAV5) and without (ACA1 to ACA5) Vp2, produced from three separate productions are given. Similar titer ranges of DNase-resistant particles were produced for all of the vector cassettes. The majority of the viral productions were found to have titers in the 1×10^7 viral genomes/μl range.

discriminate between incompletely and completely assembled virions that can effectively protect their genome from DNase I digestion and carry out a successful infection. Intact AAV particles that have assembled correctly comprise the essential topology conformation necessary to successfully bind to its cognate receptor and enter the cell, while the incompletely assembled particles may lack this ability. This allowed us to assess the genome content of infectious particles that entered the cells and released their genomes within these cells. Therefore, infection of 293 cells, made permissive for replication, with AAV2 D through L vectors was carried out as described in Materials and Methods. Approximately 40 to 42 h postinfection, the cells were harvested and low-molecular-weight DNA was isolated by following the Hirt protocol. Figure 3 (top) illustrates that the AAV2 D through L viruses can infect and deliver their respective genomes to the nuclei of 293 cells, albeit at a decreased level for the K and L vectors with respect to the others. Replicated monomer products can be detected for all of the virally delivered packaging constructs, but the replication dimer product for the L cassette is not detected at these exposure times. DNA concentrations shown on the alkaline agarose gels and quantitated by dot blots are similar between the AAV2 D through L viruses but do not correlate with the infectivity of each virus. This suggests that the K and L viral preparations may have an increased number of incompletely assembled or defective particles, protecting the larger genomes from DNase I digestion.

Based on this analysis, we carried out additional experiments on the vector packaging cassettes that appeared compromised in infectivity (i.e., cassettes E, K, and L). The next step was to purify AAV encapsidating the E, K, and L genomes via CsCl gradients and, in addition, AAV2 with iodixanol step gradients followed by FPLC-heparin column purification. AAV vectors purified under these conditions should decrease the population of incompletely assembled or defective particles from the completely assembled virions in each vector preparation, especially those encapsidating the K and L vector genomes based on binding affinity to heparin columns, density in CsCl gradients, and stability in salt. It is important to note that titers for the purified serotypes encapsidating the E, K, and L genomes were virtually equivalent (data not shown). As shown in Fig. 3 (bottom), the Southern blot of Hirt DNA isolated from representative serotypes AAV1- and AAV3 (purified from CsCl)-infected 293 cells suggests that all serotypes are capable of packaging and infecting cells with genomes as large as 6 kb. These results strongly support the viability of serotype vectors carrying genomes larger than wt size after CsCl gradient purification. The blots also indicate that the dominant species being delivered to the nucleus are full-length genomes. In agreement with the infectivity data gathered from crude lysate AAV2 infections in Fig. 3 (top), the infectivity of CsCl-purified serotypes is reduced for virions encapsidating genomes of 5.3 kb (K) and 6 kb (L). Furthermore, transmission electron micrographs of each viral preparation (Fig. 4) suggest that AAV encapsidating larger genomes are similar in size and structure to wt. Through use of this assay, it is apparent that higher proportions of empty particles are present in the AAV2 K and L viral preparations.

Analyzing CAT expression from infected cells. We next analyzed the expression levels of the CAT gene that is encoded

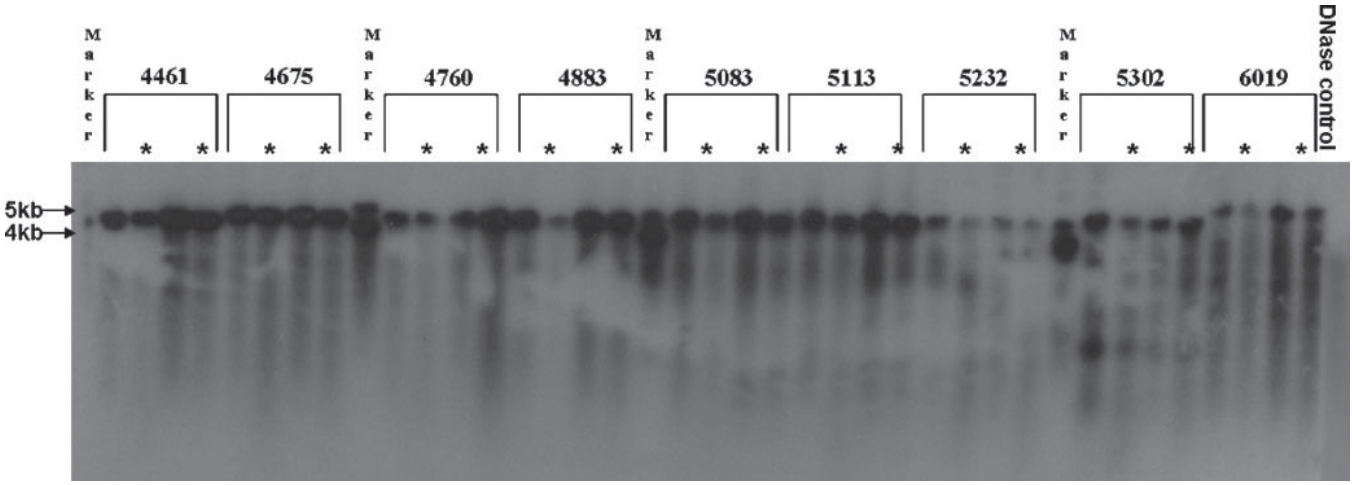

FIG. 2. Southern blot of vector DNA isolated directly from AAV virions and run on an alkaline agarose gel. The marker lanes contain DNA fragments produced from pAVCNst K cassette that are 4 kb and 5 kb in size. The DNase control lane represents the pAVCNst K cassette digested with DNase I to show that it was functional. Each set of bracketed lanes represents genomes isolated from AAV encapsidating each pAVCNst vector. The numbers above each bracketed set signify the size of the vectors. The first two lanes in each bracketed set are wt capsid, and the second set of two lanes is DNA isolated from the ACA (Vp2-less) mutants. DNase was added to the lysates of the second and fourth lanes in each bracketed set (marked with asterisks). AAV DNA was labeled with a probe specific for the CAT gene. The single-stranded vector DNAs appear as broad, blurry bands that are characteristic for AAV genomic DNA isolated from AAV capsids.

within the packaging constructs. Analyzing CAT expression from infected HeLa cells enabled us to determine the transduction profile of each serotype with and without Vp2. We chose HeLa cells for this study because, in our hands, they are transduced efficiently by AAV. HeLa cells were infected with each AAV serotype at 500 viral genomes/cell and an adenovirus MOI of 5 and harvested at 24 h postinfection. Figure 5 (top panels) shows representative transduction profiles for AAV2 and AAV4 encapsidating the CAT packaging constructs. Four to five time points were taken for each set of CAT assays, and the reactions that were in the linear range were selected for graphical representation. Variability in transfection efficiencies can result in preparation-to-preparation variation in titer and infectious-to-noninfectious particle ratios. To control for these inconsistencies, transduction assays were carried out in duplicate with separate viral preparations, and the transduction profiles depicted in Fig. 5 (top and middle panels) were found to hold true for each AAV serotype with and without Vp2. Transduction profiles from CsCl-purified AAV1 and heparin column-purified AAV2 E, K, and L are depicted in Fig. 5 (bottom panels). The heparin-purified AAV2 transduction efficiency is depicted as lower than the other profiles in Fig. 5 because this time point fell in the linear range in relation to the kinetics of the CAT reaction. The transduction profiles demonstrate that the difference in transduction efficiency between AAV packaging the wt size and the K and L genomes consistently ranged between three- to sevenfold. Based on the infectivity data represented in Fig. 3, we expected the CAT transduction profile to be lower for AAV encapsidating the K and L genomes than for genomes of wt size. We found that AAV lacking Vp2 displayed a transduction profile similar to that of AAV with all three capsid proteins (Fig. 5, middle panels). These data add more support to the previous claim that virions lacking Vp2 do not encapsidate and transduce cells with the larger genomes more efficiently. The functional relevance of Vp2 in the life cycle of AAV remains to be resolved.

Effect of proteasome inhibitors on transduction. Proteasome inhibitors have been described in numerous studies to increase the transduction of rAAV postentry of the cell, suggesting that proteasomes are a barrier for intracellular trafficking (11, 51). To help understand and potentially eliminate possibilities for why AAV encapsidating larger genomes (K and L) are not as infectious as those with genomes near wt size, we subjected each vector to various temperatures (37, 45, 56, and 65°C) for 30 min and subjected HeLa cells to various concentrations of the LLnL proteasome inhibitor prior to and at the time of infection, respectively. The AAV serotypes included in both studies were purified via CsCl gradients. The AAV2 E and K vectors were resistant to the 37 and 45°C temperatures based on transduction but were negatively affected (twofold decrease) by the 56°C temperature. The L vector was found to be more sensitive (twofold) to the 45 and 56°C temperatures than the E and K vectors, suggesting that the stability of capsids are very similar. Little to no transduction was detected with any vector when exposed to 65°C (data not shown). As shown in Fig. 6, the proteasome inhibitor improved the transduction profiles of AAV encapsidating the larger genomes to a greater extent than AAV encapsidating the wt size genome in the presence of adenovirus. Transduction profiles of AAV encapsidating the E, K, and L genomes were increased 1.1-, 2.2-, and 5.7-fold, respectively, in the presence of LLnL at a 40 μM concentration. Upon comparison of the K and L AAV1 transduction profile in the presence of the proteasome inhibitor to that of the nontreated AAV1 E, it is clear that transduction is restored to wt levels for the K vector and to near wt levels for the L vector (less than twofold difference).

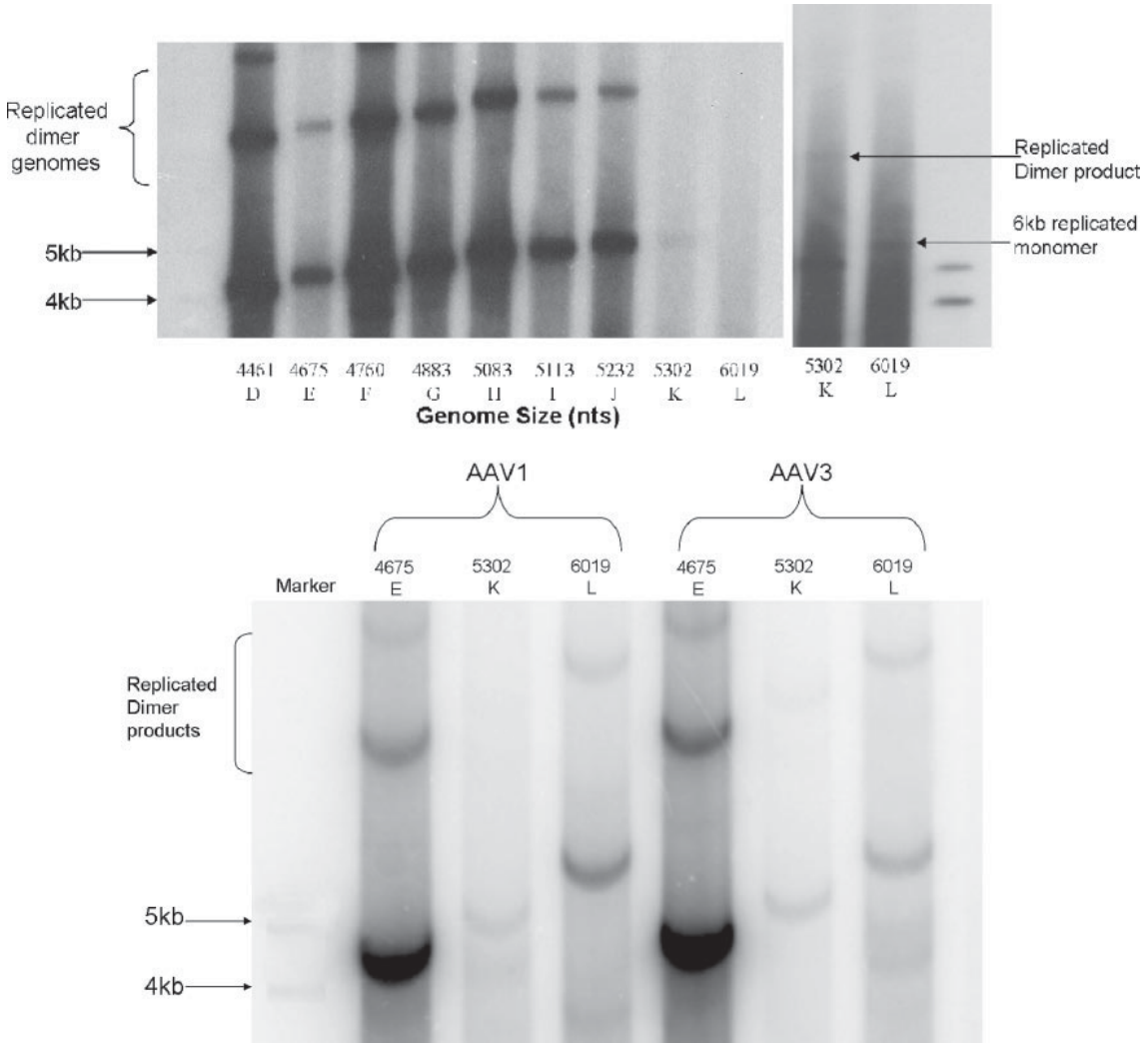

FIG. 3. (Top) Southern blot analysis of vector DNA isolated from infected 293 cells in the presence of transfected adenovirus helper (XX680) and AAV2 helper (pXR2). AAV DNA was isolated from infected 293 cells by Hirt extraction and run on a 0.7% agarose gel. AAV DNA was labeled with a probe specific for the CAT gene. The marker lanes contain DNA fragments produced from the pAVCNst K cassette that are 4 kb and 5 kb in size. Replicated dimer genomes for the 5.3- and 6-kb genomes can be detected with extended exposure times. (Bottom) Southern blot of vector DNA isolated from 293 cells infected with CsCl-purified AAV1 and 3 E, K, and L vectors in the presence of transfected adenovirus helper (XX680) and AAV2 helper (pXR2). The sizes of the E (4,675 nucleotides [nts]), K (5,302 nts), and L (6,019 nts) vector genomes are depicted at the top of the Southern blot. The correctly sized genomes and replication products are present within the cells. It is evident that the larger vectors are not as efficient in delivery as the AAV encapsidating genomes of near wt size.

Packaging full-length CFTR cassettes in AAV. To ensure the above packaging data was not unique to the CAT transgene cassettes, we tested a series of CFTR transgene cassettes for vector infectivity as described above. Three CFTR cassettes were constructed of various sizes, (i) CFTR with a TR-only promoter as previously described (5.1 kb) (21), (ii) CMV-CFTR (5.6 kb), and (iii) CMV(I)-CFTR (5.9 kb), and packaged into AAV2. The CMV(I)-CFTR construct contains a 200-bp SV40 intron (I) between the CMV promoter and the start of the CFTR gene, which has been shown to increase the gene expression of other transgenes. Each virus was characterized for its ability to package its respective genome and infect 293 cells. Figure 7 (left) shows the Southern blot of Hirt DNA isolated from infected 293 cells. It is clear that AAV is capable of encapsidating each CFTR cassette in its entirety and infecting target cells (Fig. 7, left lanes 3, 4, and 5).

Since we are not working with a reporter gene that can be easily assessed by function, as is the case for CAT, we decided to analyze each AAV2-CFTR virus' ability to transduce cells by the presence of CFTR mRNA. Briefly, HeLa cells were infected with each CFTR vector at approximately 2,000 viral genomes/cell in the presence and absence of LLnL (treatment with LLnL not shown). The poly(A) RNA was then isolated from the infected HeLa cells 48 h postinfection as described in Materials and Methods. Reverse transcription-PCR was then carried out on the isolated mRNA. Primers specific for the virally delivered CFTR transcript were then used to detect and amplify the CFTR cDNA transcripts in each sample. The

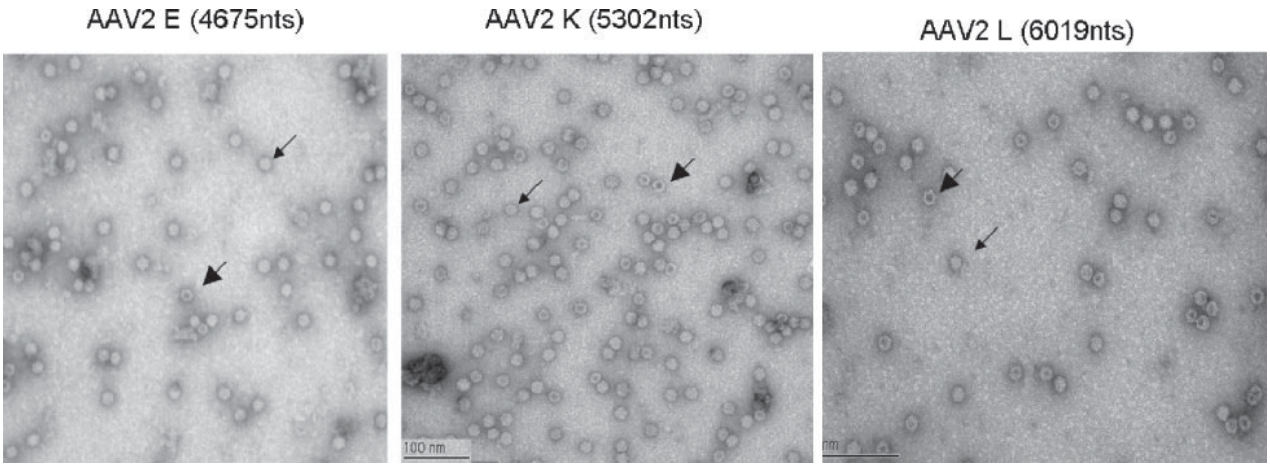

FIG. 4. Transmission electron micrographs of AAV2 E, K, and L preparations. Peak fractions of the FPLC heparin column-purified AAV2 encapsidating the E, K, and L genomes were stained in 2% uranyl acetate and imaged by transmission electron microscopy. The small arrowhead shows a genome containing rAAV2. The large arrowhead shows empty rAAV2 particles. The size and structure of each AAV vector is consistent. However, more empty particles are evident in the K and L AAV2 vector preparations. nts, nucleotides.

450-bp PCR product was successfully amplified from each sample of infected cells, suggesting that AAV is capable of transducing cell lines with CFTR cassettes as large as 5.9 kb (Fig. 7, right). A more sensitive assay, such as real-time PCR, would have to be carried out to directly compare mRNA levels between cells infected in the presence or absence of LLnL. Further studies regarding the CFTR vectors are currently ongoing but are beyond the scope of this study.

DISCUSSION

The intricate biology of AAV as a nonpathogenic human virus has led to its development into a promising viral vector for gene therapy. However, its small size has been identified as a major limitation for its use in therapies for diseases associated with larger genes, such as cystic fibrosis. Genome sizes vary among the *Parvovirus* family but are independent of capsid size. For example, the sizes of the B19, MVM, and AAV genomes are 5.6, 5.1, and 4.7 kb, respectively, encapsidated in a 25-nm capsid. What does differ structurally between these viruses is that the B19 and MVM capsids are initially composed of two capsid proteins, Vp1 and Vp2, and expose their Vp2 N termini on the surface of the capsid for further processing to Vp3 (MVM), while the Vp2 N termini of AAV are located within the virion and are not processed. The unique N terminus of Vp1 of B19 has also been described as being surface exposed (26, 34). Based on this evidence, we wanted to explore the possibility that producing a virion composed of only two capsid proteins may enable AAV to package larger genomes more efficiently than wt capsids. Our interests were threefold: to determine the packaging capacity of AAV using five different serotypes, to determine the repercussions the encapsidated larger genomes had on infectivity, and to determine whether the Vp2-deficient AAV are capable of packaging and infecting cells with larger genomes more efficiently than wt capsids.

Virus particles display considerable diversity in size, composition, and structure, ranging from those containing a single nucleic acid molecule and one structural protein to more complex structures assembled from numerous different proteins and other components. Some of these viruses have gained attention as potential vectors for human therapies, leading to numerous studies characterizing the packaging limitations of viral vectors such as adenovirus (36-kb genome), SV40 (5-kb genome), and Epstein-Barr virus (172-kb genome) (2, 3, 6). The above studies have found that packaging capacity rarely exceeds 105 to 110% of the size of the wt genome. In the case of these viruses, fitness of the larger-genome-containing viruses was tested, resulting in the identification of deletions over time. It is thought that a deletion process is being amplified by the packaging properties of each virus, leading to preferred/ideal size genomes and rescue of infectivity. In the case of this study, fitness was not tested because it is not relevant when producing vectors. The vector is only used for one round of infection and not cycled, as described in the previous studies.

A study by Brandenburger et al. characterized the packaging capacity of an autonomous parvovirus, MVM (4). The vectors utilized in this study (ranging in size from 81 to 117% of wt size) replaced part of the VP coding sequences with human interleukin-2 cDNA, keeping the NS-1 and NS-2 genes intact. Infectious particle production was best for vectors with genomes similar in size to that of wt MVM (5.1 kb). However, genomes of identical size to wt but possessing sequence foreign to wt showed dissimilar packaging efficiencies, alluding to the importance of primary viral DNA sequence and possibly its structure on packaging into the capsid. It is important to note that ordered DNA structure has been identified in crystal structures for canine parvovirus (CPV) and MVM, illustrating that the genome is bound to the interior of the capsid by a specific nucleotide-capsid interaction (1, 7, 47, 49). This concept is further reinforced by CPV structural studies showing a relationship between *cis*-acting, repeated DNA sequence motifs and specific amino acids on the capsid lumen (7). Variations of these sequence motifs were found throughout the CPV genome. However, ordered DNA has yet to be discovered in the crystal structures solved for AAV, suggesting that DNA-

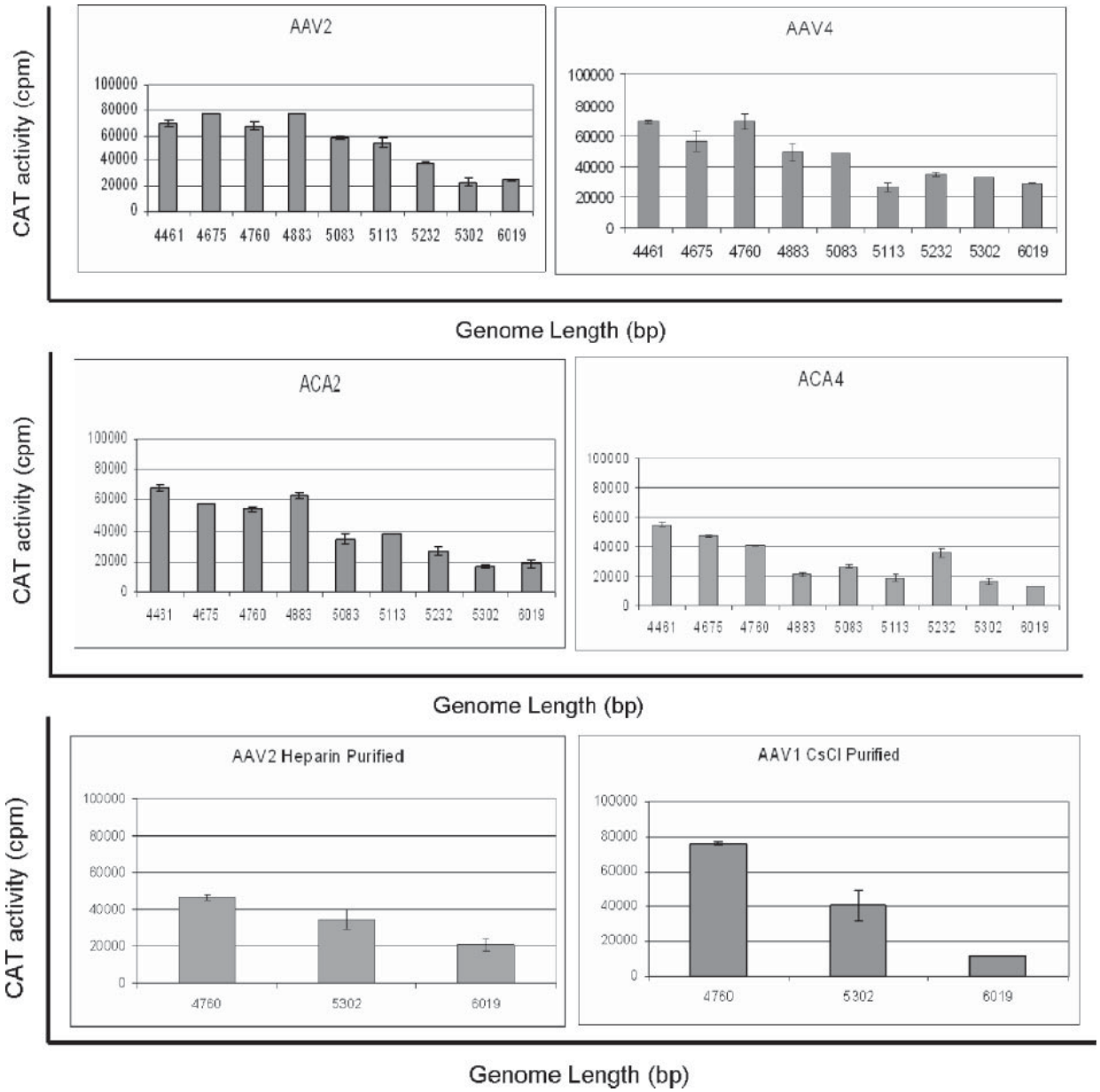

FIG. 5. Functional assay for the CAT transgene. HeLa cells (6×10^5) were infected with 500 viral genomes/cell with an adenovirus MOI of 5. Cell homogenate was collected from the HeLa cells at 24 h postinfection. CAT assays were carried out on 30 μl of protein homogenate from the infected HeLa cells. Transduction was normalized to the protein concentration for each sample. CAT activity is represented on the vertical axes in counts per minute (cpm) of radioactivity, and the horizontal axes indicate the sizes of the AAV vectors. (Top panels) Graphical representation of CAT transduction with wt capsid AAV2 and AAV4. (Middle panels) Graphical representation of CAT transduction for the Vp2-less (ACA) AAV2 and AAV4. (Bottom panels) CAT transduction profiles of CsCl-purified AAV1 E (4,675 nucleotides), K (5,302 nucleotides), and L (6,019 nucleotides) and heparin column-purified AAV2 E, K, and L. CAT activity was measured to be three- to sevenfold lower for the K and L vectors than for the E and F vectors for serotypes 1 through 5.

capsid interactions may be lacking or not as important for AAV (42, 48). It has been shown that MVM and CPV virions are dependent upon genome encapsidation for exposure of their Vp2 N termini on the surface of the capsid for subsequent proteolysis into Vp3 (1, 8, 45, 49). The nucleotide-capsid interactions seem to lead to conformational changes necessary for proper egress of the virus. AAV is not dependent on this mechanism because its genome produces the Vp3 subunit from an independent start codon. Based on our studies, it was demonstrated that AAV is capable of packaging vector genomes as large as 6 kb or approximately 130% the size of the wt genome with similar efficiency. In support of our study, a recent in vivo study by Sarkar et al. utilized AAV8 to package a 5.6-kb canine FVIII cDNA construct that was later found to give 100% correction of plasma FVIII activity in a hemophilia A mouse model (35). Although this study determined that the larger genome affected infectivity, enough vector gene product was generated to alter the diseased phenotype. With this evidence

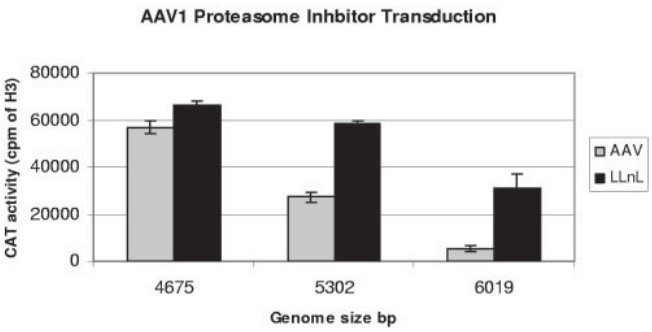

FIG. 6. CAT transduction profile of proteasome inhibitor (LLnL)-treated HeLa cells. HeLa cells (6×10^5) were infected with 500 viral genomes/cell of AAV1 E, K, and L vectors with an adenovirus MOI of 5 and 40 μM LLnL. Cell homogenate was collected from the HeLa cells at 24 h postinfection. CAT assays were carried out on 30 μl of protein homogenate from the infected HeLa cells. Transduction was normalized to the protein concentration for each sample. The gray bars represent the untreated HeLa cells, and the black bars represent HeLa cells treated with 40 μM LLnL. LLnL is shown to increase CAT activity preferentially for the K and L vectors compared to the E vector.

in hand, it is possible to hypothesize that AAV has a higher tolerance for foreign DNA because it may not be dependent on specific nucleotide-capsid interactions within the virion and in turn is capable of packaging larger genomes. However, there may be a preferred sequence context (e.g., the AAV2 genome is made up of 54% GC content), and this bias may explain previous observations of certain vector transgenes yielding higher titers than others of identical size (unpublished data).

Infectivity of AAV encapsidating larger genomes. Figure 8 shows the predicted infectious pathway of AAV2. The early steps of AAV infection involve attachment to a variety of cell surface receptors such as HSPG, FGFR, $\alpha_v\beta5$ integrin, and hepatocyte growth factor receptor (c-Met) (Fig. 8I) (9, 25, 31, 39, 40), followed by clathrin-dependent endocytosis (Fig.8II). Studies have been carried out by a number of groups (11, 22, 50, 51) illustrating that drugs/chemicals such as bafilomycin A, brefeldin A, and MG-132 augment rAAV transduction by acting on the level of endosome acidification, early-to-late endosome transition, and proteasome activity, respectively. Based on these studies, it has been proposed that AAV requires endosomal acidification to escape from the late endosome and traffic to the nucleus (Fig. 8III and IV). Use of proteasome inhibitors such as MG-132 and LLnL have been shown to increase transduction, providing evidence that after endosome escape, AAV must elude proteasomes in the cytoplasm while traversing to the nucleus (Fig. 8IV and V) (11, 51). It was recently determined that AAV capsids are ubiquitinated, marking them for degradation by the proteasome (Fig.8IV) (50), adding more support to the notion that proteasomes in the cytoplasm act as barriers to AAV infection. This study suggests that AAV is capable of encapsidating genomes as large as 6 kb with similar efficiencies as genomes of wt size (Table 1 and Fig. 2). However, these larger-genome-containing virions were found to be less infectious (within a log) than those containing genomes of wt size (Fig. 3). The inability of these viruses to infect cells efficiently was not due to their inability to bind and internalize into cells or package incomplete genomes (Fig. 3). Hirt analysis and proteasome inhibitor studies determined that the block in the infectious pathway was postentry. As depicted in Fig. 8, AAV is shown to have three potential endpoints postentry based on what is known of AAV2 intracellular trafficking. The first occurs when AAV is

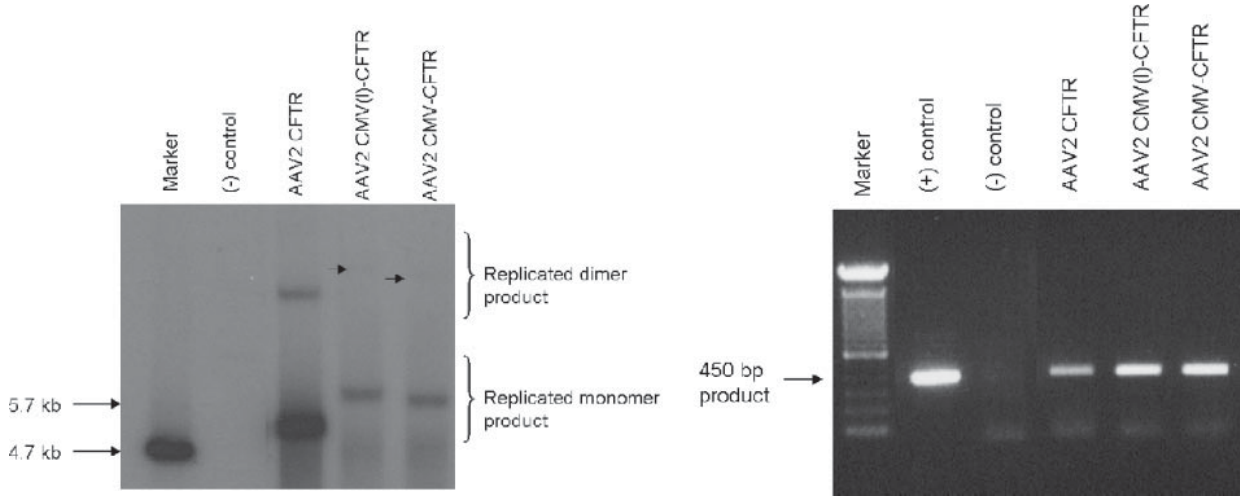

FIG. 7. (Left) Southern blot analysis of CFTR vector DNA isolated from infected 293 cells with CsCl-purified AAV2-CFTR (5.1 kb), AAV2-CMV-CFTR (5.6 kb), and AAV2-CMV(I)-CFTR (5.9 kb) virus in the presence of transfected adenovirus helper (XX680) and AAV2 helper (pXR2). CFTR vector DNA was isolated from infected 293 cells by Hirt extraction and run on a 0.7% agarose gel. CFTR vector DNA was labeled with a probe specific for the CFTR gene. Replicated monomer and dimer products can be seen for each vector at the correct size based on the 4.7- and 5.7-kb markers. The arrows present in the AAV2-CMV-CFTR and AAV2-CMV(I)-CFTR lanes represent the locations of the replicated dimer products that are present on longer exposures. (Right) Reverse transcription-PCR of poly(A) RNA isolated from AAV2-CFTR-, AAV2-CMV-CFTR-, and AAV2-CMV(I)-CFTR-infected HeLa cells. HeLa cells (5×10^5) were infected with each virus at approximately 2,000 viral genomes/cell. The poly(A) RNA was then isolated from the infected HeLa cells at 48 h postinfection as described in Materials and Methods. Primers specific for the virally delivered CFTR gene were used to detect and amplify 450 bp of the CFTR transcripts. Each CFTR vector is capable of transducing the cell line of interest.

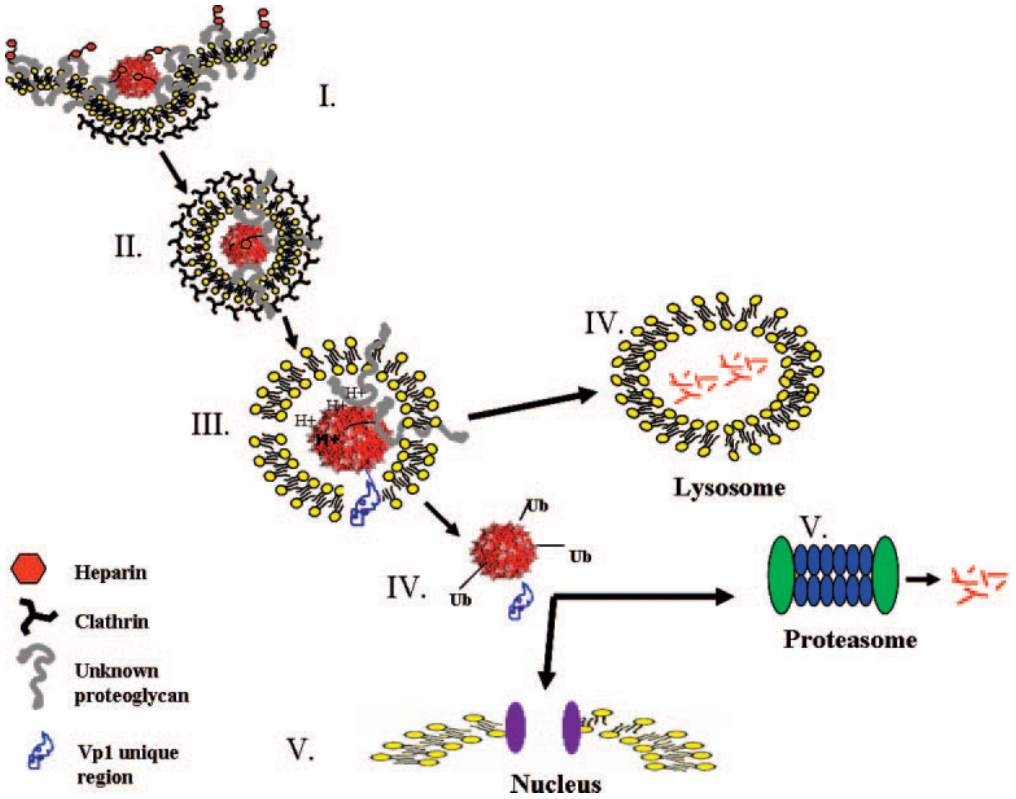

FIG. 8. Predicted model based on AAV2 trafficking. (I) The first step in AAV2 infection is binding to its primary receptor heparan sulfate proteoglycan and to a secondary receptor. (II) AAV becomes endocytosed via clathrin-coated pits and is brought into the cell in an early endosome. (III) The early endosome then matures into a late endosome as the pH begins to drop to around 5. A pH-dependent conformational change occurs that is thought to expose the N terminus of Vp1, providing the phospholipase activity aiding in endosome escape. (IV) At this point in the pathway, AAV either fails to escape the late endosome, where it later becomes degraded by the lysosome, or escapes into the cytoplasm perinuclearly, where it becomes ubiquitinated. (V) The ubiquitinated virions are then recognized by cytoplasmic proteasomes on their way to the nucleus where they are degraded, but those that avoid interaction with the proteasomes reach the nucleus for genome delivery.

unable to escape the late endosome and is routed to the lysosome for degradation (Fig. 8IV). The second and third occur after AAV has escaped from the endosome and is trafficking toward the nucleus. Data based on autonomous parvoviruses suggest that, prior to escaping the endosome, the virion is thought to undergo conformational changes, leading to the exposure of the unique N terminus of Vp1, necessary for escape (Fig. 8III) (5, 33). However, exposure of Vp1 may not be the only factor involved in escape from the endosome, as was indicated in a recent study with CPV (38). Once AAV is in the cytoplasm en route to the nucleus, the virion is thought to be ubiquitinated (Fig. 8IV), thereby being targeted for degradation by the proteasome. Those that escape degradation by the proteasome reach the nucleus and deliver their genome. Our studies using the proteasome inhibitor LLnL suggest that AAV encapsidating larger genomes are degraded at a higher frequency than those with genomes of wt size. Infectivity/transduction were restored to wt or near wt levels for AAV encapsidating the 5.3- and 6-kb genomes, respectively, shifting the balance from proteasome degradation to nuclear accumulation, resulting in increased transduction (Fig. 6). These data support the model illustrated in Fig. 8 and identify an area of AAV trafficking that will require more rigorous studies in the future.

Impact on packaging large genes. Numerous studies have addressed the issue of efficiently packaging the CFTR gene with a small promoter into AAV capsids (17, 18, 36, 43, 54). These studies identified truncated forms of CFTR that are functional when tested for activity using the patch-clamp method. Utilizing these truncated forms of CFTR in AAV vector cassettes created additional space to incorporate short promoter elements such as chicken β-acting, Rous sarcoma virus long terminal repeat, and the AAV p5 promoter while remaining close to 5 kb in size. These AAV-CFTR vectors were shown to efficiently package and deliver the CFTR transgene to the target cells displaying CFTR mRNA production and chloride channel activity. Normal levels of CFTR in airway epithelia suggest highly regulated gene expression is at play. Our studies support the possibility of constructing transgene cassettes for larger genes with a promoter of interest, such as a regulatable promoter (Fig. 7). However, a significant proportion of AAV encapsidating genomes larger than 5.2 kb appear to be targeted favorably for proteasome degradation. A combined approach utilizing proteasome inhibitors appears to be capable of reestablishing transgene expression levels for vectors greater than 5.2 kb in size to levels comparable to those encapsidating vectors of wt size. In regard to the previous studies utilizing truncated forms of CFTR, this study suggests that an additional 200 bp of DNA sequence can be incorporated into these vectors, generating AAV that will efficiently transduce cells without the aid of proteasome inhibitors.

This study suggests that AAV encapsidating genomes larger than 5.2 kb are not influenced by the presence or absence of Vp2, distinguishing autonomous parvoviruses from AAV. The addition of proteasome inhibitor at the time of infection was shown to augment transduction of the larger vectors to levels similar to AAV encapsidating vector cassettes of wt size, suggesting that the larger vectors are capable of carrying out a successful infection. These modifications can easily be adapted to current AAV vector studies and suggest that a better understanding of virus infection may lead to genetic approaches that will facilitate efficient packaging and transduction of vector transgene cassettes larger than wt size.

ACKNOWLEDGMENTS

We thank Joseph Rabinowitz, Dawn Bowles, and Doug McCarty for helpful discussion and Aravind Asokan for reviewing the manuscript. We also thank Jian-yun Dong for supplying the pAVCNst packaging cassettes used in this study.

This study was supported by NIH research grants 5P01GM059299, 2P01HL051818, 5P01HL066973, and P30 DK065988.

REFERENCES

1. **Agbandje-McKenna, M., A. L. Llamas-Saiz, F. Wang, P. Tattersall, and M. G. Rossmann.** 1998. Functional implications of the structure of the murine parvovirus, minute virus of mice. Structure **6:**1369–1381.
2. **Bett, A. J., L. Prevec, and F. L. Graham.** 1993. Packaging capacity and stability of human adenovirus type 5 vectors. J. Virol. **67:**5911–5921.
3. **Bloss, T. A., and B. Sugden.** 1994. Optimal lengths for DNAs encapsidated by Epstein-Barr virus. J. Virol. **68:**8217–8222.
4. **Brandenburger, A., E. Coessens, K. El Bakkouri, and T. Velu.** 1999. Influence of sequence and size of DNA on packaging efficiency of parvovirus MVM-based vectors. Hum. Gene Ther. **10:**1229–1238.
5. **Carreira, A., M. Menendez, J. Reguera, J. M. Almendral, and M. G. Mateu.** 2004. In vitro disassembly of a parvovirus capsid and effect on capsid stability of heterologous peptide insertions in surface loops. J. Biol. Chem. **279:**6517–6525.
6. **Chang, X. B., and J. H. Wilson.** 1986. Formation of deletions after initiation of simian virus 40 replication: influence of packaging limit of the capsid. J. Virol. **58:**393–401.
7. **Chapman, M. S., and M. G. Rossmann.** 1995. Single-stranded DNA-protein interactions in canine parvovirus. Structure **3:**151–162.
8. **Cotmore, S. F., A. M. D'Abramo, Jr., C. M. Ticknor, and P. Tattersall.** 1999. Controlled conformational transitions in the MVM virion expose the VP1 N-terminus and viral genome without particle disassembly. Virology **254:**169–181.
9. **Di Pasquale, G., B. L. Davidson, C. S. Stein, I. Martins, D. Scudiero, A. Monks, and J. A. Chiorini.** 2003. Identification of PDGFR as a receptor for AAV-5 transduction. Nat. Med. **9:**1306–1312.
10. **Dong, J. Y., P. D. Fan, and R. A. Frizzell.** 1996. Quantitative analysis of the packaging capacity of recombinant adeno-associated virus. Hum. Gene Ther. **7:**2101–2112.
11. **Douar, A. M., K. Poulard, D. Stockholm, and O. Danos.** 2001. Intracellular trafficking of adeno-associated virus vectors: routing to the late endosomal compartment and proteasome degradation. J. Virol. **75:**1824–1833.
12. **Drumm, M. L., H. A. Pope, W. H. Cliff, J. M. Rommens, S. A. Marvin, L. C. Tsui, F. S. Collins, R. A. Frizzell, and J. M. Wilson.** 1990. Correction of the cystic fibrosis defect in vitro by retrovirus-mediated gene transfer. Cell **62:**1227–1233.
13. **Duan, D., Y. Yue, and J. F. Engelhardt.** 2003. Dual vector expansion of the recombinant AAV packaging capacity. Methods Mol. Biol. **219:**29–51.
14. **Duan, D., Y. Yue, and J. F. Engelhardt.** 2001. Expanding AAV packaging capacity with trans-splicing or overlapping vectors: a quantitative comparison. Mol. Ther. **4:**383–391.
15. **Duan, D., Y. Yue, Z. Yan, and J. F. Engelhardt.** 2000. A new dual-vector approach to enhance recombinant adeno-associated virus-mediated gene expression through intermolecular cis activation. Nat. Med. **6:**595–598.
16. **Duan, D., Y. Yue, Z. Yan, and J. F. Engelhardt.** 2003. Trans-splicing vectors expand the packaging limits of adeno-associated virus for gene therapy applications. Methods Mol. Med. **76:**287–307.
17. **Flotte, T. R., S. A. Afione, C. Conrad, S. A. McGrath, R. Solow, H. Oka, P. L. Zeitlin, W. B. Guggino, and B. J. Carter.** 1993. Stable in vivo expression of the cystic fibrosis transmembrane conductance regulator with an adeno-associated virus vector. Proc. Natl. Acad. Sci. USA **90:**10613–10617.
18. **Flotte, T. R., S. A. Afione, R. Solow, M. L. Drumm, D. Markakis, W. B. Guggino, P. L. Zeitlin, and B. J. Carter.** 1993. Expression of the cystic fibrosis transmembrane conductance regulator from a novel adeno-associated virus promoter. J. Biol. Chem. **268:**3781–3790.
19. **Girod, A., C. E. Wobus, Z. Zadori, M. Ried, K. Leike, P. Tijssen, J. A. Kleinschmidt, and M. Hallek.** 2002. The VP1 capsid protein of adeno-associated virus type 2 is carrying a phospholipase A2 domain required for virus infectivity. J. Gen. Virol. **83:**973–978.
20. **Haberman, R. A., G. Kroner-Lux, and R. J. Samulski.** 1999. Production of recombinant adeno-associated viral vectors. Curr. Protoc. Hum. Genet. **23**(Suppl.)**:**12.9.1–12.9.17.
21. **Haberman, R. P., T. J. McCown, and R. J. Samulski.** 2000. Novel transcriptional regulatory signals in the adeno-associated virus terminal repeat A/D junction element. J. Virol. **74:**8732–8739.
22. **Hansen, J., K. Qing, and A. Srivastava.** 2001. Adeno-associated virus type 2-mediated gene transfer: altered endocytic processing enhances transduction efficiency in murine fibroblasts. J. Virol. **75:**4080–4090.
23. **Hermonat, P. L., J. G. Quirk, B. M. Bishop, and L. Han.** 1997. The packaging capacity of adeno-associated virus (AAV) and the potential for wild-type-plus AAV gene therapy vectors. FEBS Lett. **407:**78–84.
24. **Jones, N., and T. Shenk.** 1979. Isolation of adenovirus type 5 host range deletion mutants defective for transformation of rat embryo cells. Cell **17:**683–689.
25. **Kashiwakura, Y., K. Tamayose, K. Iwabuchi, Y. Hirai, T. Shimada, K. Matsumoto, T. Nakamura, M. Watanabe, K. Oshimi, and H. Daida.** 2005. Hepatocyte growth factor receptor is a coreceptor for adeno-associated virus type 2 infection. J. Virol. **79:**609–614.
26. **Kawase, M., M. Momoeda, N. S. Young, and S. Kajigaya.** 1995. Most of the VP1 unique region of B19 parvovirus is on the capsid surface. Virology **211:**359–366.
27. **Kronenberg, S., J. A. Kleinschmidt, and B. Bottcher.** 2001. Electron cryomicroscopy and image reconstruction of adeno-associated virus type 2 empty capsids. EMBO Rep. **2:**997–1002.
28. **Lusby, E., K. H. Fife, and K. I. Berns.** 1980. Nucleotide sequence of the inverted terminal repetition in adeno-associated virus DNA. J. Virol. **34:**402–409.
29. **McCarty, D. M., S. M. Young, Jr., and R. J. Samulski.** 2004. Integration of adeno-associated virus (AAV) and recombinant AAV vectors. Annu. Rev. Genet. **38:**819–845.
30. **Muralidhar, S., S. P. Becerra, and J. A. Rose.** 1994. Site-directed mutagenesis of adeno-associated virus type 2 structural protein initiation codons: effects on regulation of synthesis and biological activity. J. Virol. **68:**170–176.
31. **Qing, K., C. Mah, J. Hansen, S. Zhou, V. Dwarki, and A. Srivastava.** 1999. Human fibroblast growth factor receptor 1 is a co-receptor for infection by adeno-associated virus 2. Nat. Med. **5:**71–77.
32. **Rabinowitz, J. E., F. Rolling, C. Li, H. Conrath, W. Xiao, X. Xiao, and R. J. Samulski.** 2002. Cross-packaging of a single adeno-associated virus (AAV) type 2 vector genome into multiple AAV serotypes enables transduction with broad specificity. J. Virol. **76:**791–801.
33. **Reguera, J., A. Carreira, L. Riolobos, J. M. Almendral, and M. G. Mateu.** 2004. Role of interfacial amino acid residues in assembly, stability, and conformation of a spherical virus capsid. Proc. Natl. Acad. Sci. USA **101:**2724–2729.
34. **Rosenfeld, S. J., K. Yoshimoto, S. Kajigaya, S. Anderson, N. S. Young, A. Field, P. Warrener, G. Bansal, and M. S. Collett.** 1992. Unique region of the minor capsid protein of human parvovirus B19 is exposed on the virion surface. J. Clin. Investig. **89:**2023–2029.

34a. **Sambrook, J., and D. W. Russell.** 2001. Molecular cloning: a laboratory manual, 3rd ed. Cold Spring Harbor Laboratory Press, Cold Spring Harbor, N.Y.

35. **Sarkar, R., R. Tetreault, G. Gao, L. Wang, P. Bell, R. Chandler, J. M. Wilson, and H. H. Kazazian, Jr.** 2004. Total correction of hemophilia A mice with canine FVIII using an AAV 8 serotype. Blood **103:**1253–1260.
36. **Sirninger, J., C. Muller, S. Braag, Q. Tang, H. Yue, C. Detrisac, T. Ferkol, W. B. Guggino, and T. R. Flotte.** 2004. Functional characterization of a recombinant adeno-associated virus 5-pseudotyped cystic fibrosis transmembrane conductance regulator vector. Hum. Gene Ther. **15:**832–841.
37. **Srivastava, A., E. W. Lusby, and K. I. Berns.** 1983. Nucleotide sequence and organization of the adeno-associated virus 2 genome. J. Virol. **45:**555–564.
38. **Suikkanen, S., M. Antila, A. Jaatinen, M. Vihinen-Ranta, and M. Vuento.** 2003. Release of canine parvovirus from endocytic vesicles. Virology **316:**267–280.
39. **Summerford, C., J. S. Bartlett, and R. J. Samulski.** 1999. AlphaVbeta5 integrin: a co-receptor for adeno-associated virus type 2 infection. Nat. Med. **5:**78–82.
40. **Summerford, C., and R. J. Samulski.** 1998. Membrane-associated heparan sulfate proteoglycan is a receptor for adeno-associated virus type 2 virions. J. Virol. **72:**1438–1445.
41. **Sun, L., J. Li, and X. Xiao.** 2000. Overcoming adeno-associated virus vector size limitation through viral DNA heterodimerization. Nat. Med. **6:**599–602.
42. **Walters, R. W., M. Agbandje-McKenna, V. D. Bowman, T. O. Moninger, N. H. Olson, M. Seiler, J. A. Chiorini, T. S. Baker, and J. Zabner.** 2004. Structure of adeno-associated virus serotype 5. J. Virol. **78:**3361–3371.
43. **Wang, D., H. Fischer, L. Zhang, P. Fan, R. X. Ding, and J. Dong.** 1999.

Efficient CFTR expression from AAV vectors packaged with promoters—the second generation. Gene Ther. **6:**667–675.
44. **Warrington, K. H., Jr., O. S. Gorbatyuk, J. K. Harrison, S. R. Opie, S. Zolotukhin, and N. Muzyczka.** 2004. Adeno-associated virus type 2 VP2 capsid protein is nonessential and can tolerate large peptide insertions at its N terminus. J. Virol. **78:**6595–6609.
45. **Weichert, W. S., J. S. Parker, A. T. Wahid, S. F. Chang, E. Meier, and C. R. Parrish.** 1998. Assaying for structural variation in the parvovirus capsid and its role in infection. Virology **250:**106–117.
46. **Wobus, C. E., B. Hugle-Dorr, A. Girod, G. Petersen, M. Hallek, and J. A. Kleinschmidt.** 2000. Monoclonal antibodies against the adeno-associated virus type 2 (AAV-2) capsid: epitope mapping and identification of capsid domains involved in AAV-2-cell interaction and neutralization of AAV-2 infection. J. Virol. **74:**9281–9293.
47. **Wu, H., and M. G. Rossmann.** 1993. The canine parvovirus empty capsid structure. J. Mol. Biol. **233:**231–244.
48. **Xie, Q., W. Bu, S. Bhatia, J. Hare, T. Somasundaram, A. Azzi, and M. S. Chapman.** 2002. The atomic structure of adeno-associated virus (AAV-2), a vector for human gene therapy. Proc. Natl. Acad. Sci. USA **99:**10405–10410.
49. **Xie, Q., and M. S. Chapman.** 1996. Canine parvovirus capsid structure, analyzed at 2.9 A resolution. J. Mol. Biol. **264:**497–520.
50. **Yan, Z., R. Zak, G. W. Luxton, T. C. Ritchie, U. Bantel-Schaal, and J. F. Engelhardt.** 2002. Ubiquitination of both adeno-associated virus type 2 and 5 capsid proteins affects the transduction efficiency of recombinant vectors. J. Virol. **76:**2043–2053.
51. **Yan, Z., R. Zak, Y. Zhang, W. Ding, S. Godwin, K. Munson, R. Peluso, and J. F. Engelhardt.** 2004. Distinct classes of proteasome-modulating agents cooperatively augment recombinant adeno-associated virus type 2 and type 5-mediated transduction from the apical surfaces of human airway epithelia. J. Virol. **78:**2863–2874.
52. **Yan, Z., Y. Zhang, D. Duan, and J. F. Engelhardt.** 2000. Trans-splicing vectors expand the utility of adeno-associated virus for gene therapy. Proc. Natl. Acad. Sci. USA **97:**6716–6721.
53. **Zadori, Z., J. Szelei, M. C. Lacoste, Y. Li, S. Gariepy, P. Raymond, M. Allaire, I. R. Nabi, and P. Tijssen.** 2001. A viral phospholipase A2 is required for parvovirus infectivity. Dev. Cell **1:**291–302.
54. **Zhang, L., D. Wang, H. Fischer, P. D. Fan, J. H. Widdicombe, Y. W. Kan, and J. Y. Dong.** 1998. Efficient expression of CFTR function with adeno-associated virus vectors that carry shortened CFTR genes. Proc. Natl. Acad. Sci. USA **95:**10158–10163.
55. **Zolotukhin, S., B. J. Byrne, E. Mason, I. Zolotukhin, M. Potter, K. Chesnut, C. Summerford, R. J. Samulski, and N. Muzyczka.** 1999. Recombinant adeno-associated virus purification using novel methods improves infectious titer and yield. Gene Ther. **6:**973–985.